Influence of fine particle peening treatment on various characteristics of Ti–Ni shape memory alloys

Koichiro NAMBU [a], Noboru EGAMI [b]
[a] Toyota Technological Institute, Japan, knambu@toyota-ti.ac.jp
[b] Institution, country, egami@meijo-u.ac.jp

Keywords: Shape memory alloys, Fine Particle Peening, Fatigue strength, Micro Structure

Introduction

Ti–Ni shape-memory alloy (SMA) is an alloy exhibiting a shape-memory effect and a super-elastic effect because of the occurrence of martensitic and rhombohedral phases. SMAs are widely used in small actuators and drive elements of robots. In recent years, several studies have been conducted on the biocompatibility of SMAs and their use in medical devices. Accordingly, it is necessary to understand the change in the characteristics associated with the accumulation of fatigue damage in SMAs employed in high-cycle applications. So far, studies have been conducted on rotational bending-fatigue characteristics and compression-fatigue characteristics of SMAs [1–7].

However, when used for medical devices and the like, an allergy is induced because of the dissolution of Ni ions contained in SMAs. Hence, the surface is modified via particular treatments to improve the corrosion resistance and biocompatibility. In conventional studies, it has been reported that an amorphous structure is formed near the surface when treated with strong processing techniques such as the shot-peening treatment and fine-particle peening (FPP) treatment [8–10]. Furthermore, elution of Ni ions from the amorphous structure can be suppressed [11, 12]. However, studies on evaluating the fatigue property of SMAs using surface-modification treatments have not been conducted.

In this study, the effects of the FPP treatment on the shape memory effect and fatigue strength characteristics of an SMA, which has been effective in improving the fatigue strength in steel materials [13–16], were investigated.

Methodology

Ti-50% Ni alloy was used for the experiment. After preparing the specimen, shown in Fig. 1, the specimen was polished with a waterproof abrasive paper up to # 2000. Thereafter, after holding for 1 h at 773 K, furnace cooling was performed. The specimens were FPP treated was performed on the specimens after heat treatment under the conditions listed in Table 1. The Young's modulus and Vickers hardness measurement, structure observation, and X-ray diffraction measurement were conducted on the untreated material and specimens after peening to analyze the surface-modification effect.

The Young's modulus and hardness were measured using a nano-indentation method. Table 2 lists the measurement conditions. The surface modified layer and inside of the structure were analyzed to investigate the corrosion resistance. To observe the structure, an etching solution, presented in Table 3, was used and the structure was studied under an electron microscope. The X-ray diffraction measurement was conducted under the conditions listed in Table 4. In the measurement, the untreated martensite phase was used as a comparative material.

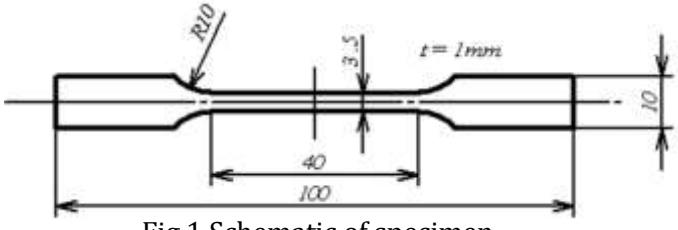

Fig.1 Schematic of specimen

Table 1 FPP conditions

Shot material	High speed steel Ceramic
Diameter of shot (μm)	50
Air pressure (MPa)	0.6
Process time (Sec)	30

Thereafter, the tensile experiment, training experiment, and tensile fatigue experiment were conducted and their influences on the repetitive characteristics and fatigue-strength characteristics were investigated. Tables 5 and 6 list the respective experimental conditions. The training experiment is conducted to understand the repeated deformation characteristics of the SMA using the hysteresis loop in the stress–strain diagram by repeated loading and unloading.

Table 2 Nano-indentation and hardness measurement

Indenter	Vickers
Maximum load (mN)	50
Loading time (Sec)	10
Holding time (Sec)	20
Unloading time (Sec)	10

Table 3 Etching solution

Nitric acid	6
Hydroflouric acid	3
Water	1

Table 4 X-ray conditions

Method	Parallel beam method
Characteristic X-ray	Cr-Kα
Filter	V
Tube voltage (kV)	40
Tube current (mA)	30
Scanning speed (deg/min)	1
Time constant (Sec)	10
High angle	160°
Low angle	20°

Table 5 Condition of training experiment

Crosshead speed (mm/min)	0.1
Cycles of stressed (cycle)	100

Table 6 Condition of fatigue experiment

Repeatedly speed (Hz)	8
Stress amplitude	0.05
Factor of stress concentration	1.19

Results and discussion

Result of Young's modules measurement

Fig. 2 shows the measurement results of the Young's modulus in the depth direction. As shown in the figure, in the FPP treated material, the Young's modulus near the surface increases by approximately 30 GPa as compared to the untreated material. As reported in previous studies, it is conceivable that the vicinity around the surface is transformed into nano-crystallized or amorphous form because of the high strain observed during the FPP treatment.

Result of hardness measurement

Fig. 3 shows the hardness measurement results in the depth direction. The figure shows that the hardness near the surface is largely increased because of the FPP treatment, as observed in the measurement of the Young's modulus. The hardness of the untreated material is approximately 400 HV, whereas that of the FPP treated material increases to approximately 600 MPa. Moreover, the effective depth is approximately 20 μm, as observed in the measurement result of the Young's modulus. This is because of the work hardening due to the high strain generated near the surface similar to the increase in the Young's modulus.

Result of structure observation

Fig. 4 shows the SEM images of the cross section of the specimens. Figs. 4(a), 4(b), and 4(c) show the images for the cases of no etching, an etching time of 30 s, and an etching time of 60 s. Fig. 4 (a) shows that a structure different from that of the inside was formed up to approximately 15 μm from the surface. The Young's modulus and hardness-measurement show that this structure is an amorphous structure or a nanocrystal structure. The Young's modulus and hardness-measurement result show that the structure is not uniform up to the depth of 20 μm and its value is decreasing. Thus, this region is not only amorphous but also exhibits an inclined structure having amorphous-to-nanocrystals and fine crystals. Next, the results in Figs. 4(b) and 4(c) show that the progress of the corrosion via the etching is slower in the affected layer than in the inside. Thus, the corrosion resistance of the structure obtained via the FPP treatment is high. This result is consistent with the results obtained by Wang et al. [17].

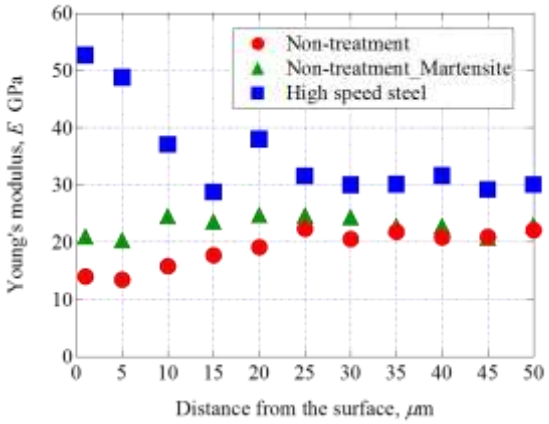

Fig. 2 Distribution of Young's modules

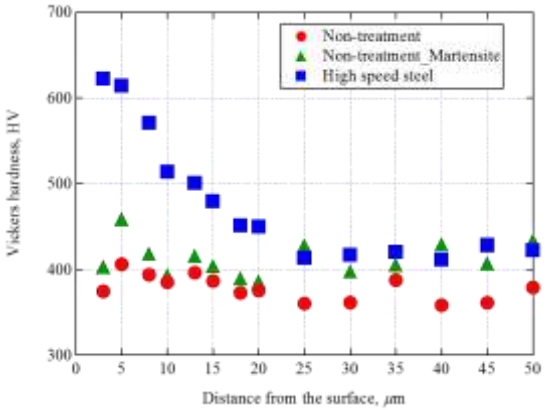

Fig. 3 Distribution of hardness

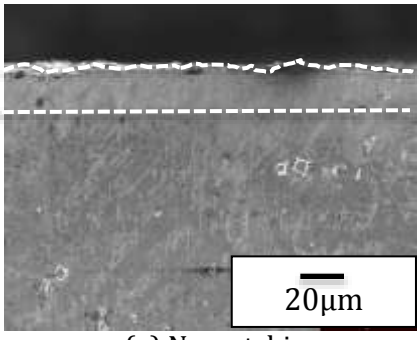

(a) Non-etching

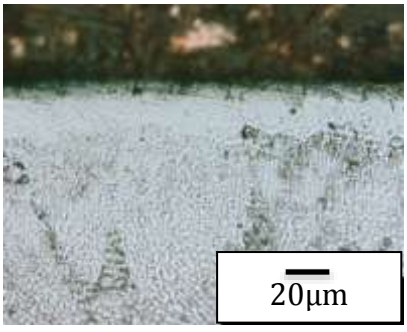

(b) 30Sec

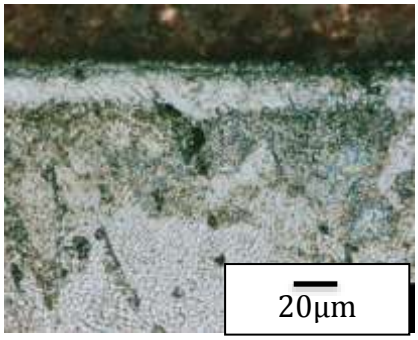

(c) 60Sec

Fig. 4 Observation of structure

Result of X-ray diffraction measurement

Fig. 5 shows the results of the X-ray diffraction measurement. The figure shows that there is a large difference in the diffraction intensity depending on whether the FPP treatment is employed. Peaks were observed in the martensitic structure of the untreated material and untreated material, whereas no peak was detected in the FPP material. Moreover, this tendency is consistent with the results obtained by Kikuchi et al. [9]. Further, because the penetration depth of X-rays is approximately 10 μm, it is considered that the amorphous layer is formed up to approximately 10 μm.

Result of tensile experiment

Fig. 6 shows the results for the untreated and FPP materials. In Fig. 6(a), the FPP treated and untreated specimens are compared. Fig. 6(b) shows the result of the influence of the projection pressure. Because of the treatment, the stress required to initiate the martensitic transformation and stress during transformation tend to increase. As this factor, in addition to the amorphous and microcrystalline layers formed near the surface, the influence of the residual strain is considered. The results in Fig. 6 (b) show that the stress rise differs depending on the projection pressure. It is also found that the stress rises as the projection pressure increases.

Result of fatigue experiment

Fig. 7 shows the fatigue experiment results. This result shows that an increase in the hardness helps in significantly improving the fatigue strength on the higher-cycle side regardless of the shot material in the FPP material. In addition, it is considered that the improvement in the fatigue strength via improvement of the hardness could not be obtained due to the stress concentration due to increase in surface roughness as a factor of not showing the effect of improving the fatigue strength on the high stress side.

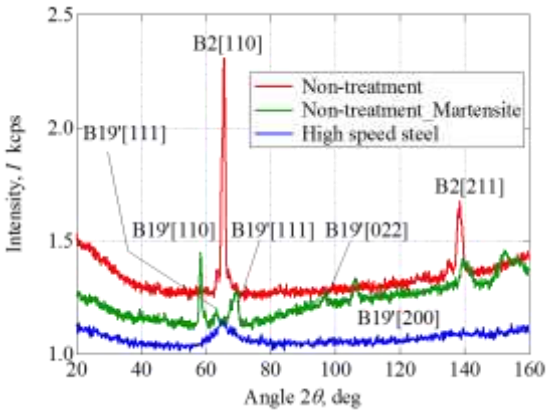

Fig. 5 X-ray diffraction

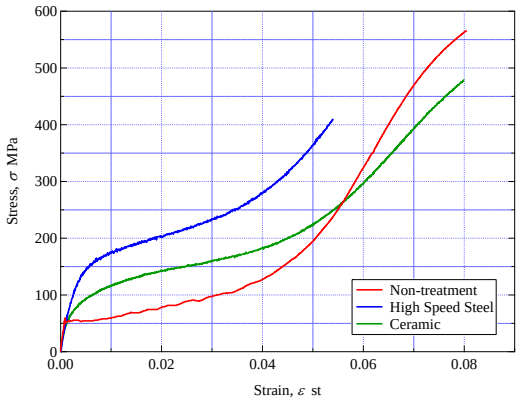

Fig. 6 (a) Influence of FPP on tensile strength

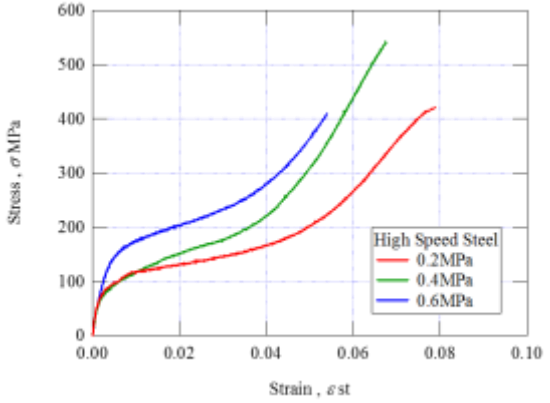

Fig. 6 (b) Influence of shot pressure on tensile strength

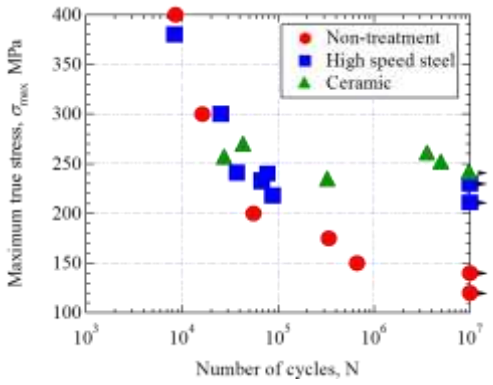

Fig. 7 Result of Fatigue experiment

Result of training experiment

Figs. 8 and 9 show the result of the training experiment. The figure shows that the fracture occurred at 50 cycles for the untreated material, whereas for the FPP material, the specimen did not rupture even at 100 cycles. As the number of cycles of the SMA increases, the recovery amount tends to decrease. Thus, the growth and disappearance of the martensitic phase occurs in the loading and unloading processes in the SMA. Simultaneously, the interface between the martensite phase and the mother layer moves repeatedly. Therefore, internal stress due to the dislocation and residual strain is generated at the interface. Because the internal stress helps the transformation to proceed, transformation occurs even with a small amount of stress. This shows that the tendencies in both the FPP material and untreated material are similar. However, the amount of change in this recovery is smaller in the FPP-treated material. This is because of the influence of the compressive residual stress generated during the FPP treatment in addition to the influence of the internal stress mentioned previously. In addition, it is considered that the rupture did not occur because of the increase in the hardness. The results of the fatigue and training experiments show that the FPP treatment is effective in improving the strength of the SMA.

Influence of FPP processing on the inside of specimen

Next, to investigate the influence of the amorphous layer on the surface, electro polishing was performed on the specimen after the FPP treatment, and a training experiment was performed on the specimens from which the amorphous layer was removed. Fig. 9 shows the results. As shown in the figure, the hysteresis loop of the electro-polished FPP material is similar to that of the untreated material, thereby making it clear that the influence of the amorphous layer was the main factor that helped in improving the strength in the FPP treatment.

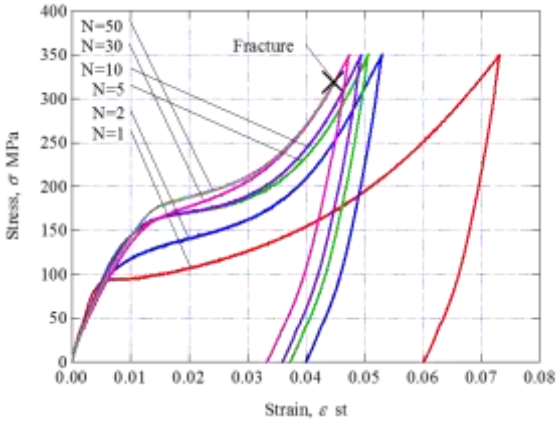

Fig.8 (a) Training experiment result of Non-treatment

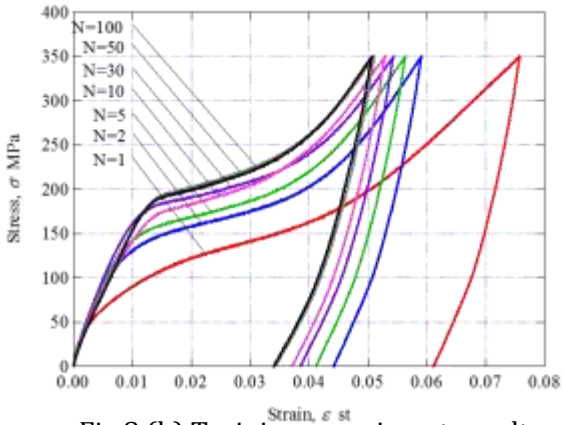

Fig.8 (b) Training experiment result of FPP specimen

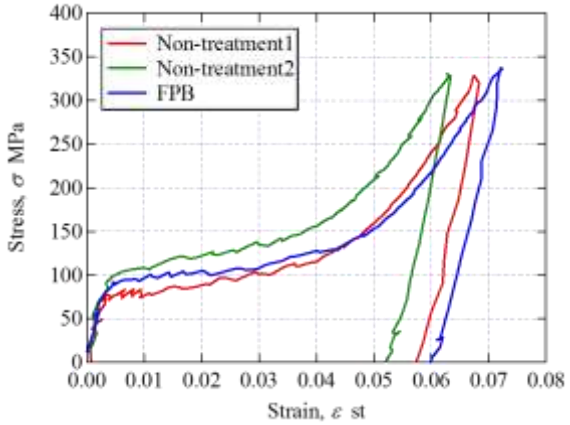

Fig.9 Influence of removal of surface layer on stress-strain curve

Conclusions

The following conclusions can be drawn from the studies on high performance and high strength of Ti–Ni SMA via fine particle-peening treatment:

1. The transformation stress can be controlled by changing the FPP-treatment condition
2. By applying the FPP treatment, it is possible to improve the life and strength while having the same shape-recovery performance as the untreated material.
3. The influence of the FPP treatment was limited to the surface of the specimen, and it was revealed that the amorphous layer helped in improving the strength.

References

[1] N.B. Morgan: Material Science Engineering A378 (2004) 16-23
[2] Namazu T, Hashizume A, Inoue S, Sens Actuators A 139(2007), 178
[3] H. Tobushi, P.H.Lin, A. Ikai and S. Yamada, Journal of Japan Society of Mechanical Engineering, 591 (1995), 517 (in Japanese)
[4] H. Tobushi, P.H.Lin, T. Hattori and M. Makita, Journal of Japan Society of Mechanical Engineering, 562 (1995), 517 (in Japanese)
[5] D. J. Wever, A. G. Veldhuizen, D. R. A.Uges, J. R. Vanhon, J. De Vries and H. J. Busscher, Biomaterials, 19, 7-9(1998)761
[6] S. A. Shabalovskaya, Biomedical Material Engineering, 6 (1996), 267
[7] J. Ryhanen, Minimally Invasive Therapy and allied Technology, 9 (1982), 99
[8] C. Ye, S. Suslov, X. Fei, and G. J. Chang, Acta Materials 59 (2011), 7219
[9] S. Kikuchi, M, Mizutani, Y, Kameyama and J. Komotori, journal of the Japan Society for Abrasive Technology 57(2013), 530 (in Japanense)
[10] Q. Cao, K. Tuchiya, Y. Harada, D. Tomus, K. Morii, Y. Todaka and M. Umemoto, Journal of Japan Institute of Metals and Materials, 70 (2006), 473 (in Japanese)
[11] R. W. Y. Poon, K. W. K. Yeung, M. Y. Liu, P. K. Chu, C. Y. Chung, W. Lu, K. M. C. Cheung and D. Chan, Biomaterials, 26 15(2005), 2265
[12] R. W. Y. Poon, P. Y. H. Joan, M. Y. Luk Camille, X. Liu, C. Y. C. Jonathan, K. C. Paul, W. Y. Kelvin, W. L. William and M. C. C. Kenneth, Nuclear Instruments and Methods in Physics research B, 242, 1-2(2006), 270
[13] D. Yonekura, J. Komotori, M. Shimizu and H. Shimizu, Journal of The Surface Finishing Society of Japan, 53 (2002). 214(in Japanese)
[14] K. Nambu and N. Egami, Fracture and Structural Integrity, 34(2015), 271-279
[15] S. Kikuchi, Y. Hirota and J. Komotori, Journal of the Society of Materials Science, Japan, 60, 6(2011) 547-553(in Japanese)
[16] S. Kikuchi, Y. Nakamura, K. Nambu and M. Ando, Material Science & Engineering A, 652(2016). 279-286
[17] X. Y. Wang, D. Y. Li, Wear, 255, 7-12(2003), 836